blood advances

The human IL-15 superagonist ALT-803 directs SIV-specific CD8$^+$ T cells into B-cell follicles

Gabriela M. Webb,[1,2,*] Shengbin Li,[3,*] Gwantwa Mwakalundwa,[3] Joy M. Folkvord,[4] Justin M. Greene,[1,2] Jason S. Reed,[1,2] Jeffery J. Stanton,[2] Alfred W. Legasse,[2] Theodore Hobbs,[2] Lauren D. Martin,[2] Byung S. Park,[2] James B. Whitney,[5,6] Emily K. Jeng,[7] Hing C. Wong,[7] Douglas F. Nixon,[8] R. Brad Jones,[8] Elizabeth Connick,[4] Pamela J. Skinner,[3] and Jonah B. Sacha[1,2]

[1]Vaccine and Gene Therapy Institute and [2]Oregon National Primate Research Center, Oregon Health & Science University, Portland, OR; [3]Department of Veterinary and Biomedical Sciences, University of Minnesota, St. Paul, MN; [4]Division of Infectious Diseases, University of Arizona, Tucson, AZ; [5]Center for Virology and Vaccine Research, Beth Israel Deaconess Medical Center, Harvard Medical School, Boston, MA; [6]Ragon Institute of MGH, MIT, and Harvard, Cambridge, MA; [7]Altor BioScience Corporation, Miramar, FL; and [8]Department of Microbiology Immunology and Tropical Medicine, The George Washington University, Washington, DC

Key Points

- IL-15 superagonist sends antiviral CD8 T cells to B-cell follicles, which typically exclude them.

Sequestering of latent HIV in follicular helper T cells within B-cell follicles that largely exclude cytotoxic T cells is a major barrier to cellular immune-based approaches to eradicate HIV. Here, we show that the clinical-grade human interleukin-15 (IL-15) superagonist ALT-803 activates and redirects simian immunodeficiency virus (SIV)–specific CD8$^+$ T cells from the peripheral blood into B-cell follicles. In agreement with the increased trafficking of SIV-specific cytotoxic T cells to sites of cryptic viral replication, lymph nodes of elite controlling macaques contained fewer cells expressing SIV RNA or harboring SIV DNA post–ALT-803 treatment. These data establish ALT-803 as an immunotherapeutic for HIV and other chronic viral pathogens that evade host immunity by persisting in B-cell follicles.

Introduction

Virus-specific CD8$^+$ T cells are predominantly excluded from B-cell follicles.[1-4] Viral pathogens like HIV and Epstein-Barr virus exploit this anatomic segregation to establish persistent reservoirs in CD4$^+$ follicular helper T (T$_{FH}$) cells and B cells, respectively, residing within the B-cell follicle. In HIV elite controllers and antiretroviral therapy (ART)-treated patients, T$_{FH}$ cells are the major source of persistent HIV.[5,6] Accordingly, the development of therapeutic strategies that induce virus-specific CD8$^+$ T cells capable of infiltrating into the B-cell follicle to eliminate reactivated latently HIV-infected T$_{FH}$ is a major unmet goal of shock-and-kill approaches for achieving an immune-mediated HIV cure.

The common γ-chain cytokine interleukin-15 (IL-15) is a critical regulator of natural killer (NK) and T-cell homeostasis, and thus is an ideal candidate for clinical immunotherapy. In contrast to other γ-chain cytokines, such as IL-2 and IL-7, that circulate as soluble protein until they bind their receptor directly on target immune cells, IL-15 first binds the IL-15 receptor α-chain (IL-15Rα) for subsequent presentation in trans to target cells, thereby limiting the therapeutic use of free IL-15. Thus, the IL-15 superagonist ALT-803 was created to circumvent this limitation of IL-15 and to advance IL-15:IL-15Rα−based therapies into the clinic.[7] ALT-803 consists of a human IgG1 Fc fused onto 2 IL-15Rα units, each bound to an IL-15 superagonist monomer variant, IL-15$_{N72D}$, which exerts fivefold higher activity than wild type IL-15.[8] Together, these modifications provide ALT-803 with 25-fold higher biological activity and a 35-fold longer half-life in serum compared with free IL-15.[9] We previously demonstrated that ALT-803 is well tolerated in both mice and cynomolgus macaques to ≤100 μg/kg and does not induce a global cytokine storm despite potently activating NK and memory T cells.[8] Given this safety profile and promising results in cancer immunotherapy, we explored whether ALT-803 might be effective in the setting of established chronic viral infections using SIV-infected macaques.

The full-text version of this article contains a data supplement.

Methods

Reagents, animals, and veterinary procedures

All rhesus macaques (RMs) (*Macaca mulatta*) and Mauritian cynomolgus macaques (*Macaca fascicularis*) used in this study were housed at the Oregon National Primate Research Center and used for studies under the approval of the Oregon Health and Science University Institutional Animal Care and Use Committee. All macaques in this study were managed according to the Oregon National Primate Research Center animal care program, which is fully accredited by Association for Assessment and Accreditation of Laboratory Animal Care International and is based on the laws, regulations, and guidelines set forth by the US Department of Agriculture (eg, the Animal Welfare Act and its regulations and the Animal Care Policy Manual), the Institute for Laboratory Animal Research (eg, Guide for the Care and Use of Laboratory Animals, 8th edition), and the Public Health Service Policy on Humane Care and Use of Laboratory Animals. Whenever possible, and while still adhering to the Institutional Animal Care and Use Committee mandate to minimize animal usage, in vivo studies were repeated in a second, separate cohort of macaques. Specifically, the 5-bromo-2′-deoxyuridine (BrdU) incorporation and SIV-specific T-cell homing to B-cell follicle studies were each performed in 2 distinct cohorts of animals. The IL-15 superagonist ALT-803 was generated by Altor BioScience as previously described.[6] All ALT-803 injections were given as IV bolus doses of either 6 µg/kg or 100 µg/kg. For BrdU injections, BrdU was suspended at 10 mg/mL in Hanks balanced salt solution (HyClone Laboratories, Logan, UT) and then injected IV in the saphenous vein at a rate of 2 to 3 mL/minute for a total dose of 60 mg/kg of BrdU.

Blood and tissue processing

Whole blood was collected into EDTA-treated tubes (BD Biosciences, San Jose, CA). Blood was assessed for complete blood counts using an ABX Pentra 60 C+ analyzer (Horiba, Irvine, CA). Bronchoalveolar lavage fluid was filtered through 70-µm strainers before staining. Bone marrow was pelleted by centrifugation at 830*g* for 4 minutes and then resuspended and vigorously shaken in 1× phosphate-buffered saline (PBS) containing 2 nM EDTA to disassociate large cell clumps. Colons and livers were diced into 5-mm pieces, and 25 to 30 of these pieces were placed in a 50-mL conical containing 25 mL RPMI 1640, supplemented with 3% fetal calf serum (FCS) (R3; Hyclone Laboratories). Dithiothreitol was added at a final concentration of 200 µM, and tissues were shaken at 225 rpm for 15 min at room temperature. Tissues were allowed to settle, and the R3 with dithiothreitol was aspirated and replaced with R3 containing 5 mM EDTA. Tissues were shaken at 225 rpm for 30 minutes at 37°C, and the cell-containing supernatant was collected and passed through a cell strainer. R3 containing EDTA was added again, tissues were shaken, and the cells collected. Tissues were washed 3 times in 1× Hanks balanced salt solution to remove excess EDTA and then were suspended in R3 containing 0.2 mg/mL collagenase (Sigma-Aldrich, St. Louis, MO) and 0.2 mg/mL DNase I (Roche, Indianapolis, IN). Tissues were shaken at 225 rpm for 1 hour at 37°C, and the cell-containing supernatant was collected and passed through a metal strainer. Cell fractions collected from the EDTA and collagenase digestion steps were combined (total tissue) and resuspended in 70% isotonic Percoll (GE Healthcare, Buckinghamshire, United Kingdom). The cells were then underlayed in 37% Percoll gradient and spun at 500*g* with the brake off. Mononuclear cells from the lower interface were collected and washed in RPMI 1640 containing 10% FCS (R10). Lymph node and spleen were diced with scalpels and then forced through a 70-µm cell strainer. The strainer was rinsed repeatedly with R10 to obtain a single-cell suspension. Immune cell phenotyping was conducted on whole-blood samples that were washed twice in 1× PBS and then surface-stained for 30 minutes at room temperature. Samples were then incubated in 1 mL FACSLyse for 10 minutes, spun at 830*g* for 4 minutes, and washed 3 times in 1× PBS, supplemented with 10% FCS (fluorescence-activated cell sorter buffer). For Ki67 assessment, fixed cells were washed twice in 1 mg/mL saponin (saponin buffer) and stained overnight at 4°C. For BrdU assessment, fixed cells were washed twice in a 1:1 mixture of saponin buffer and 2× BD FACSPerm, then washed once in saponin buffer, and stained for 1 hour at room temperature in the presence of 0.5 mg/mL DNase I. After staining, samples were washed twice in saponin buffer and then run on an LSR II (Becton Dickinson, Franklin Lakes, NJ). Flow cytometric data were analyzed using FlowJo, version 10 (TreeStar, Ashland, OR). An example gating strategy is shown in supplemental Figure 9.

Carboxyfluorescein succinimidyl ester proliferation assay

Cells were labeled with carboxyfluorescein succinimidyl ester (CFSE) cell tracer (Thermo Fisher Scientific, Waltham, MA) in PBS. Cells were then stimulated for 7 days with 10-fold dilutions of ALT-803 (10 pM, 100 pM, 1 nM, 10 nM, 100 nM, and 1 uM), Staphylococcal enterotoxin B, or media alone. At the end of the stimulation, cells were washed and stained for viability with an amine-reactive dye and stained for CD3, CD8, and CD4. Data were acquired via flow cytometry as described above.

IFN-γ enzyme-linked immunospot analysis

Responses against SIV open reading frame (ORF) peptide pools were tested in an interferon-γ (IFN-γ) enzyme-linked immunosorbent spot assay using fresh peripheral blood mononuclear cells (PBMCs). Peptides were tested in duplicate wells at a concentration of 10 µg/mL or 10 µM (either individually or in pools) with 100 000 PBMCs per well. The total numbers of spots for duplicate wells were averaged, and all the numbers of spots were normalized to the numbers of IFN-γ spot-forming cells per 1×10^6 PBMCs. Responses comprising <50 spot-forming cells per 10^6 cells were considered negative and were not tested statistically. Positive responses were determined by using a 1-tailed Student *t* test and an α level of 0.05, where the null hypothesis was that the background level would be greater than or equal to the treatment level. If determined to be positive statistically, the values were reported as the average of the test wells minus the average of all negative control wells.

T-cell stimulation and intracellular cytokine staining assay

SIV-specific CD8+ and CD4+ T-cell responses were measured in PBMC preparations from the blood by flow cytometric intracellular cytokine staining assay. PBMCs were incubated with either Gag peptide pool or a mixture of Rev, Tat, and Nef peptide pools in addition to the costimulatory molecules CD28 and CD49d (BD Biosciences), for 1 hour, followed by the addition of Brefeldin A
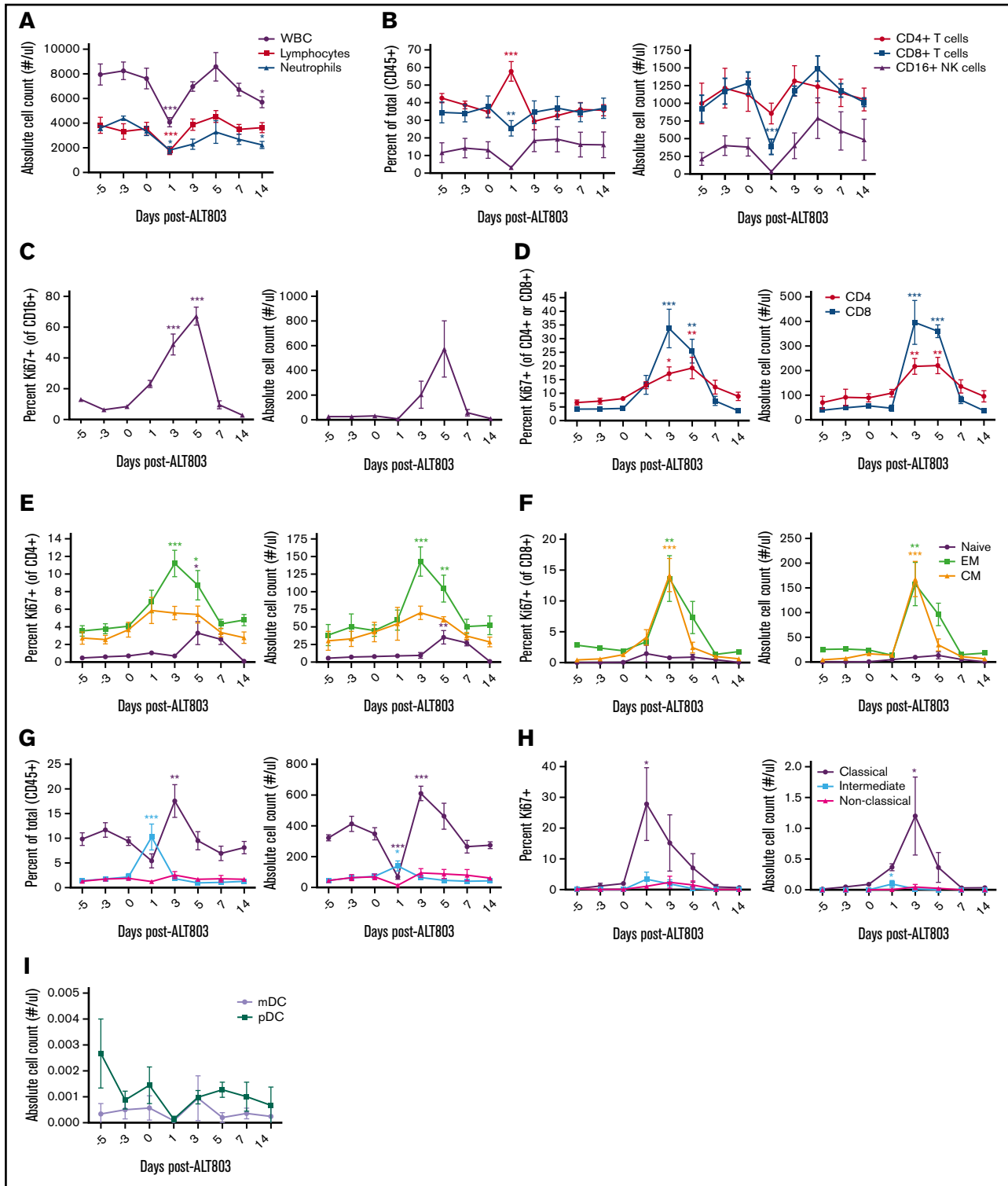
Figure 1. In vivo administration of ALT-803 in SIV-naive RMs. SIV-naive RMs (n = 4) were injected IV at day 0 with 6 μg/kg of ALT-803. Blood was collected before injection and at days 1, 3, 5, 7, and 14 postinjection. (A) White blood cell (WBC) count, lymphocytes, and neutrophils as well as (B) CD4^{+} T cell, CD8^{+} T cells, and CD16^{+} NK cells were analyzed from the blood. Proliferation of (C) CD16^{+} NK cells, (D) CD4^{+} and CD8^{+} T cells as well as naive, effector memory (EM) and central memory (CM) populations of (E) CD4^{+} and (F) CD8^{+} T-cell subsets determined as a percentage of Ki67^{+} cells of that particular lymphocyte population. (G) Whole blood was further evaluated for classical monocytes (CD14^{+}, CD16^{−}), intermediate monocytes (CD14^{+}, CD16^{+}), and nonclassical monocytes (CD14^{−}, CD16^{+}) as a percentage of CD45^{+} cells. (H) Proliferation of monocyte subsets was determined as a percentage of Ki67^{+} cells of that particular population. (I) Absolute counts of myeloid dendritic cells (mDC, defined as Lin^{−}, HLA-DR^{+}, CD11c^{+}) and plasmacytoid dendritic cells (pDC, defined as Lin^{−}, HLA-DR^{+}, CD123^{+}) were also determined. Absolute counts were calculated

(Sigma-Aldrich) for an additional 8 hours. Stimulated cells were surface-stained for CD4 and CD8. For intracellular stains (CD3, tumor necrosis factor-α, and IFN-γ), cells were washed twice with 1× fluorescence-activated cell sorter buffer, fixed in 2% paraformaldehyde and subsequently washed in saponin buffer. Cells were then stained for 1 hour at room temperature. After staining, cells were washed in saponin buffer and analyzed via flow cytometry as described above.

Quantitative real-time reverse transcriptase polymerase chain reaction

PBMCs were sorted for $CD8\beta^+$ T cells via magnetic sorting using a phycoerythrin-conjugated anti-CD8β antibody (clone 2ST8.5H7, Beckman Coulter) and anti-phycoerythrin MicroBeads (Miltenyi Biotec). Purified cells were resuspended in R10 and incubated with or without 10 nM ALT803. Cells were subsequently collected at days 1, 3, and 5, and RNA was extracted using the AllPrep DNA/RNA mini kit (Qiagen). Relative quantitative real-time reverse transcriptase polymerase chain reaction (RT-PCR) was performed using AgPath-ID One-Step RT-PCR reagents (Thermo Fisher Scientific). Primer pairs for the detection of rhesus CXCR5 and internal β-actin control were as follows: CXCR5 (forward, 5′-TTCACCTCCCGATTCCTCTA-3′; reverse, 5′-CAACCTGTG CACTACCCC-3′), and β-actin (forward, 5′-ATGCTTCTAGGCG GACTGTG-3′; reverse, 5′-AAAGCCATGCCAATCTCATC-3′). The TaqMan probe sequence for CXCR5 was 5′-GGATTC CTGCTGCCCATGCT-3′, and for β-actin, the probe sequence was 5′-TGCGTTACACCCTTTCTTGACAAAACC-3′. Both probes were labeled at the 5′ end with a 5′ 6-carboxyfluorescein and a 3′ black hole quencher-1 (BHQ-1). The Applied Biosystems StepOnePlus Real-Time PCR System (Thermo Fisher Scientific) was used for real-time polymerase chain reaction analysis. Thermal cycling conditions were designed as follows: initial denaturation at 95°C for 10 minutes, followed by 40 cycles of 95°C for 15 seconds and 60°C for 45 seconds. RNA levels in all samples were relative to the housekeeping gene, β-actin.

In situ tetramer staining combined with immunohistochemistry

In situ tetramer staining combined with immunohistochemistry was performed on fresh lymph tissue specimens shipped overnight, sectioned with a compresstome, and stained essentially as previously described.[1] Biotinylated peptide-loaded major histocompatibility complex (MHC)-class I monomers for Mamu-A1*001:01 Gag$_{181-189}$CM9, Mamu-A1*002:01 Nef$_{159-167}$YY9, and Mamu-B*08:01 Nef$_{137-146}$RL10 (National Institutes of Health Tetramer Core Facility, Emory University, Atlanta GA) were converted to fluorescein isothiocyanate-labeled MHC-class I tetramers. Fresh lymph node sections were incubated with MHC-class I tetramers (0.5 μg/mL) and rat–anti-human CD8 antibody (2 μg/mL, clone YTC182.20, Acris). For secondary incubations, sections were incubated with (1) rabbit–anti-fluorescein isothiocyanate Abs (0.5 μg/mL, BioDesign, Saco, ME) and mouse–anti-human CD20 Abs (0.19 μg/mL, clone L26, Novocastra), or (2) mouse-anti–human CD20 Abs (0.19 μg/mL, clone L26, Novocastra) and

rat-anti–human CD3 Abs (2 μg/mL, clone CD3-12, BioRad). For the tertiary incubations, all sections were incubated with Cy3-conjugated goat–anti-rabbit Abs (0.3 μg/mL, Jackson Immuno-Research Laboratories), Alexa Fluor 488–conjugated goat–anti-mouse Abs (0.75 μg/mL, Molecular Probes), and Cy5-conjugated goat–anti-rat Abs (0.3 μg/mL, Jackson ImmunoResearch Laboratories). Sections were imaged using a Zeiss LSM 800 confocal microscope. Montage images of multiple 512 × 512 pixels were created and used for analysis. Confocal z-series were collected in a step size of 1.23 μm.

Quantification of SIV-specific CD8 T cells in situ

Images were opened and analyzed in Image J software (National Institutes of Health) directly. Follicular areas were identified morphologically as clusters of brightly stained, closely aggregated $CD20^+$ cells. Follicular and extrafollicular areas were delineated and measured using Image J software. Areas that showed loosely aggregated B cells that were ambiguous as to whether the area was a follicle were not included. To prevent bias, the red tetramer channel was turned off until follicular and extrafollicular areas were delineated. Cell counts were done on single z-scans. In each animal, an average of 815 tetramer$^+$ cells (range, 197-2127) in follicular regions and 1755 (range, 326-4762) in extrafollicular regions were analyzed. An average of 17.2 mm^2 (range 7.8-32.8 mm^2) was evaluated for each lymph node.

Detection and quantification of SIVmac239 RNA–producing cells in lymphoid tissue

SIVmac239 RNA–producing cells were detected on 5-μm thick formalin fixed paraffin embedded sections of lymph node using RNAscope technology (Advanced Cell Diagnostics [ACD], Newark, CA). Briefly, fresh cut sections were dewaxed in Xylene, subjected to epitope unmasking by heating in citrate buffer (ACD, treatment 2), protease treated (ACD), and incubated with an SIVmac239 probe for 2 hours at 40°C. The RNAscope 2.5 detection kit with FastRed was used to amplify and detect the probe. Sections were counterstained by blocking with 1% normal donkey serum (The Jackson Laboratory, Bar Harbor, ME) and 0.5% casein (Vector Laboratories, Burlingame, CA) in Tris-buffered saline and staining with rabbit–anti-CD20 (Abcam, Cambridge, MA) to identify follicles, followed by secondary staining with Alexa Fluor 647–labeled donkey–anti-rabbit IgG (Invitrogen). Sections were counterstained with 4′,6-diamidino-2-phenylindole (DAPI), mounted in Slowfad Diamond Antifade (Invitrogen), and scanned at 40× on an Aperio Versa 8 scanner (Leica Biosystems). Aperio Image Scope (version 12.3.2.5030, Leica Biosystems) was used to quantify virus-producing cells and measure total and follicular areas. For each lymph node, 4 separate sections (each a minimum of 30 μm apart) were analyzed. The total area analyzed was a median of 23.2 mm^2 (range, 19.5-51.5 mm^2). The individuals performing the analysis were blinded to the treatment status of the animals.

Statistics

The repeated-measures analysis of variance test was used for all longitudinal studies. Paired Student t test (2 sided) was used for

---

Figure 1. (continued) based on the percentage of the particular cell subset and the WBC count. Data shown are means (± standard errors of the means) of combined data from all 4 animals. *$P < .05$; **$P < .01$; ***$P < .001$ comparing time points to time point zero.
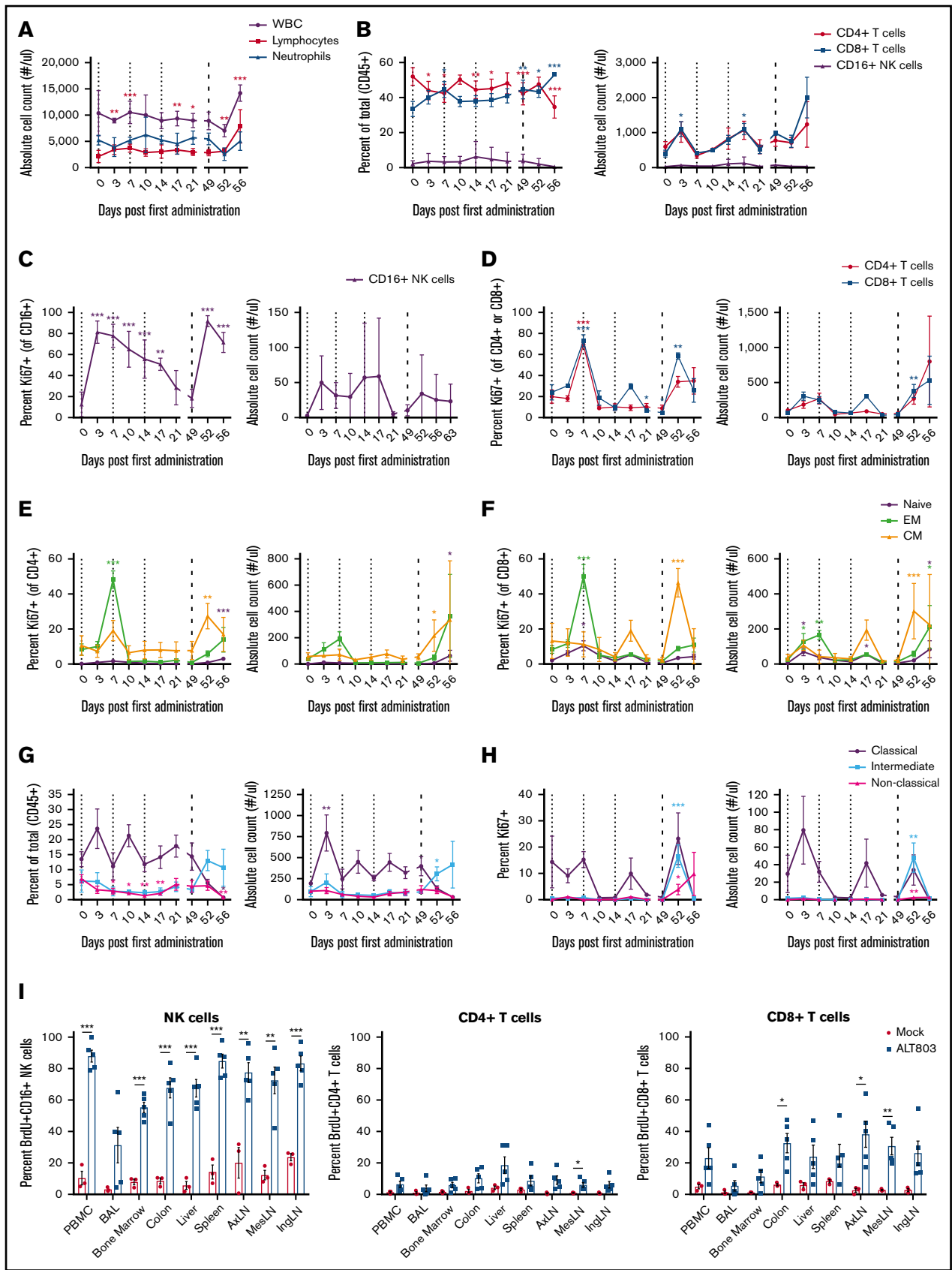
Figure 2.

all other analyses. Statistical analyses were conducted using GraphPad Prism software version 6.0 (GraphPad Software, La Jolla, CA). The statistical significance of the findings was set at $P < .05$.

Results

We first titrated ALT-803 on macaque PBMCs and found that cells displayed maximum proliferation when treated with ≥ 1 nM ALT-803, suggesting 1 nM as the minimum target serum concentration (supplemental Figure 1). We administered 1 IV injection of 6 μg/kg ALT-803, estimated by allometric scaling to be equivalent to 1 nM in blood,[8] to 4 SIV-naive RMs. One-day posttreatment with ALT-803, the absolute numbers of blood CD4+ T cells, CD8+ T cells and CD16+ NK cells decreased, followed by a rebound between days 3 and 5, concomitant with significant increases in the expression of the proliferation marker Ki-67 (Figure 1A-D). In agreement with previous reports of the effect of free IL-15 on T-cell populations in nonhuman primates,[10,11] effector memory T cells proliferated to the highest levels in response to ALT-803 (Figure 1E-F). ALT-803 also increased both the absolute number and the activation status of classical CD14+CD16− blood monocytes with no impact on dendritic cell subsets (Figure 1G-I).

To examine the effects of repeated ALT-803 dosing in SIV+ macaques, we next treated 4 SIV-infected RMs with 3 weekly IV doses of 6 μg/kg ALT-803, followed by an IV dose of 100 μg/kg after a 5-week resting period. Mirroring the effect in SIV-naive RMs, ALT-803 induced proliferation in CD4+ and CD8+ T cells and CD16+ NK cells in the blood after the first 6-μg/kg dose and again after the final 100-μg/kg dose (Figure 2A-D). We observed activation of classical blood monocytes after these doses (Figure 2G-H). Interestingly, the 100-μg/kg dose activated additional cellular subsets, including intermediate CD14+CD16+ monocytes and central memory T cells in the blood (Figure 2E-H). Despite the activation and expansion of T cells after ALT-803 administration, we observed no consistent, statistically significant changes in the magnitude of SIV-specific T-cell responses in the blood over time as measured by intracellular cytokine staining (ICS) and whole−SIV proteome IFN-γ ELISPOT assays (supplemental Figure 2A-C). After the 100-μg/kg dose, we detected a trend of increased frequency and absolute counts of SIV-specific MHC-I tetramer+ CD8+ T cells in the blood, which was corroborated by increased expression of Ki67 in these cells (supplemental Figure 2D-E). We observed no consistent changes in plasma viral loads and no adverse effects of ALT-803 treatment at any dose as assessed clinically or by serum chemistry (supplemental Figures 2F and 3A).

ALT-803 administration in both SIV-naive and SIV-infected macaques resulted in an immediate, but transient decrease in blood lymphocytes (Figure 1A; supplemental Figure 4A). Thus, we next sought to determine the anatomical location of these proliferating cells. We injected 5 SIV-infected RMs with 100 μg/kg ALT-803, leaving 3 SIV-infected RMs untreated as controls, and administered BrdU to all 8 RMs. Five days after treatment with ALT-803, we found that both NK cells and T cells proliferated, as measured by BrdU incorporation, localizing predominantly in secondary lymphoid tissues (Figure 2I). Indeed, we noted marked lymphadenitis in all animals post−ALT-803, mainly due to infiltrating CD8+ T cells (Figure 3A). Given that ALT-803 triggered an influx of CD8+ T cells into the lymph node posttreatment, we next examined the frequency of SIV-specific MHC-I tetramer+ CD8+ T cells in the lymph node compared with the peripheral blood of SIV-infected progressor (n = 3) or controller (n = 3) RMs. In the controller RMs, defined as animals that control virus <10 000 copies/mL plasma, ALT-803 again induced the expansion of NK and T cells in the peripheral blood as described above, with no consistent changes in serum chemistry values (supplemental Figures 3B and 4). Interestingly, the controller RM with detectable plasma viremia experienced a transient ∼1-log reduction in viral loads (supplemental Figure 5) post−ALT-803. There was a trend toward increased numbers of SIV-specific CD8+ T cells in the peripheral blood, but it did not reach statistical significance (Figure 3B). In contrast, there was a marked and statistically significant increase of SIV-specific CD8+ T cells within the lymph nodes post−ALT-803.

A major hurdle in the eradication of HIV is the shielding of infected CD4+ T$_{FH}$ cells from virus-specific CD8+ T cells within lymph node B-cell follicles.[5] We next measured whether ALT-803 treatment affected the expression of the B-cell follicle homing molecule CXCR5 and subsequent anatomical distribution of T cells within the lymph nodes. CD8+ T cells exposed to ALT-803 in vitro exhibited a 50-fold increase in *CXCR5* messenger RNA and a corresponding increase in surface expression of CXCR5 (Figure 3C-D). Based on these data, we performed in situ SIV-specific MHC-I tetramer staining of lymph node sections from 6 SIV-infected RMs (progressor, n = 3; controller, n = 3) immediately before and 5 days after administering 100 μg/kg ALT-803. Counterstaining for CD8 and CD20 allowed for quantification of numbers and spatial localization of SIV-specific CD8+ T cells in relation to B-cell follicles. As previously described,[1] SIV-specific CD8+ T cells localized predominantly in the extrafollicular space in the lymph nodes of SIV-infected RMs before treatment (Figure 4A). However, after ALT-803 treatment, the total number of SIV-specific CD8+ T cells within the lymph nodes increased dramatically, with significant accumulation

---

Figure 2. In vivo administration of ALT-803 in SIV-infected RMs. (A-G) SIV-infected RMs (n = 4) were injected IV with 6 mg/kg ALT-803 at days 0, 7, and 14 (indicated by thin dashed lines) and subsequently with 100 mg/kg ALT-803 at day 49 (indicated by thick dashed line). (A) White blood cell (WBC), lymphocytes, and neutrophils as well as (B) CD4+ T cells, CD8+ T cells, and CD16+ NK cells were longitudinally evaluated in the peripheral blood. Proliferation of (C) CD16+ NK cells, (D) CD4+ and CD8+ T cells as well as of naive, effector memory (EM), and central memory (CM) populations of (E) CD4+ T cell and (F) CD8+ T-cell subsets were determined as a percentage of Ki-67+ cells of that particular lymphocyte population. (G) Whole blood was evaluated for classical monocytes (CD14+CD16−), intermediate monocytes (CD14+CD16+), and nonclassical monocytes (CD14−CD16+) as a percentage of CD45+ cells. (H) Proliferation of monocyte subsets was determined as a percentage of Ki67+ cells of that particular population. Absolute counts were calculated based on the percentage of the particular cell subset and the WBC count. Data shown are means (± standard errors of the means) of combined data from 4 animals. (I) SIV-infected RMs were injected IV with BrdU (60 mg/kg) and 100 mg/kg ALT-803 (n = 5) or PBS (n = 3). Animals were then taken to necropsy 5 days later. CD16+ NK cells, CD4+ T cells, and CD8+ T cells were assessed for BrdU incorporation in the peripheral blood (PBMC), bronchoalveolar lavage (BAL) fluid, bone marrow, colon, liver, spleen, axillary lymph nodes (AxLN), mesenteric lymph nodes (MesLN), and inguinal lymph nodes (IngLN). *P < .05; **P < .01; ***P < .001 comparing time points to time point zero.
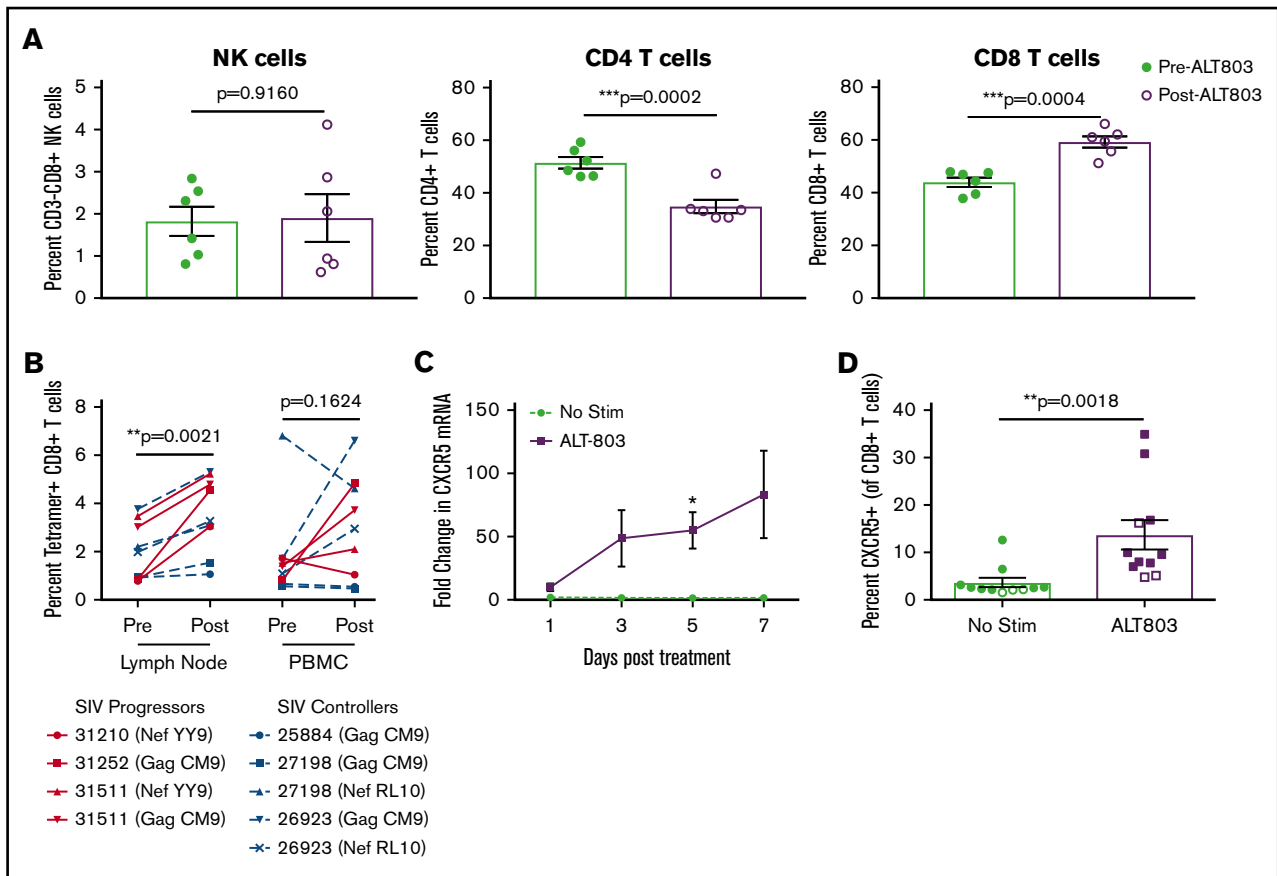
Figure 3. ALT-803 drives SIV-specific CD8^{+} T cells to lymph nodes in vivo and triggers upregulation of CXCR5 in vitro. SIV-infected RMs received 100 µg/kg of ALT-803. Lymph nodes were sampled before ALT-803 treatment and 5 days posttreatment. (A) The percentage of CD3-CD8^{+} NK cells, CD4^{+} T cells, and CD8^{+} T cells were determined in single-cell suspensions derived from AxLN before and after treatment with 100 µg/kg ALT-803. (B) Percent of SIV-specific CD8^{+} T cells as measured by MHC class I tetramer staining in lymph nodes and PBMCs. Animal identification numbers and MHC-I tetramer used are indicated. SIV progressors (n = 3) are indicated by solid red lines, and SIV controllers (n = 3) are indicated by dashed blue lines. (C) CD8β-sorted T cells from 6 RMs were cultured in vitro for 7 days with or without 15 nM ALT-803 and CXCR5 messenger RNA levels were determined via quantitative RT-PCR at days 1, 3, 5, and 7 posttreatment. (D) PBMCs from 9 RMs (filled) and 3 cynomolgus macaques (open) were cultured in vitro for 5 days with or without 15 nM ALT-803. CD8^{+} T cells were then assessed for surface expression of CXCR5. *$P < .05$; **$P < .01$; ***$P < .001$.

within B-cell follicles (Figure 4B-C). This infiltration of SIV-specific CD8^{+} T cells into B-cell follicles normalized the distribution of antiviral CD8^{+} T cells between the follicular and extrafollicular space (Figure 4D). In accordance with the presence of increased anti-viral effector CD8^{+} T cells in follicles, lower numbers of SIV-producing cells were found within the B-cell follicles of the controller RMs, with lower cell-associated DNA levels in CD4^{+} T cells, after ALT-803 treatment (Figure 4E; supplemental Figures 6 and 7), demonstrating that ALT-803 does not cause an increase in the viral reservoir as opposed to the other common γ-chain cytokines, IL-2 and IL-7.[12,13]

Discussion

ALT-803, a novel IL-15 superagonist, is a potent alternative to IL-15 immunotherapy in the setting of cancer, displaying increased immunostimulatory activity and prolonged serum half-life.[8,9,14,15] These findings have recently been extended to HIV infection, where ALT-803-activated NK cells inhibit acute HIV infection in vivo,[16] and ALT-803 also reactivates latent virus in vitro.[17] In this study, we demonstrated that ALT-803 significantly enhanced lymphocyte proliferation and activation, specifically CD16^{+} NK cells and

memory CD4^{+} and CD8^{+} T cells both in vitro and in vivo in SIV-naive and SIV-infected RMs. The slight differences in the kinetics of cellular activation and proliferation between SIV-naive and SIV-infected RMs could be due to ongoing immune activation, immune exhaustion, or viremia itself. Nevertheless, these differences were minor compared with the ability of ALT-803 to perturb the immune system. Although we observed a substantial increase in the proliferation of SIV-specific CD8^{+} T cells, there was no significant change in T-cell frequencies in the peripheral blood, likely due to the migration of these cells into effector sites, such as the mucosa. Although it remains possible that other mechanisms, such as T cell exhaustion, may also play a role, our data are in line with other recent reports of IL-15–induced migration of memory T cells out of the peripheral blood into tissue.[18]

It is well established that CD8^{+} T cells are predominantly excluded from B-cell follicles,[1-4,19] and that during HIV and SIV infection, these lymph node follicles become sanctuary sites for viral replication by avoiding antiviral CD8^{+} T cells.[5] In the absence of virus-specific CD8^{+} T-cell surveillance, B-cell follicles are thus established as long-lasting sites of the HIV and SIV viral reservoir. We demonstrate here that ALT-803
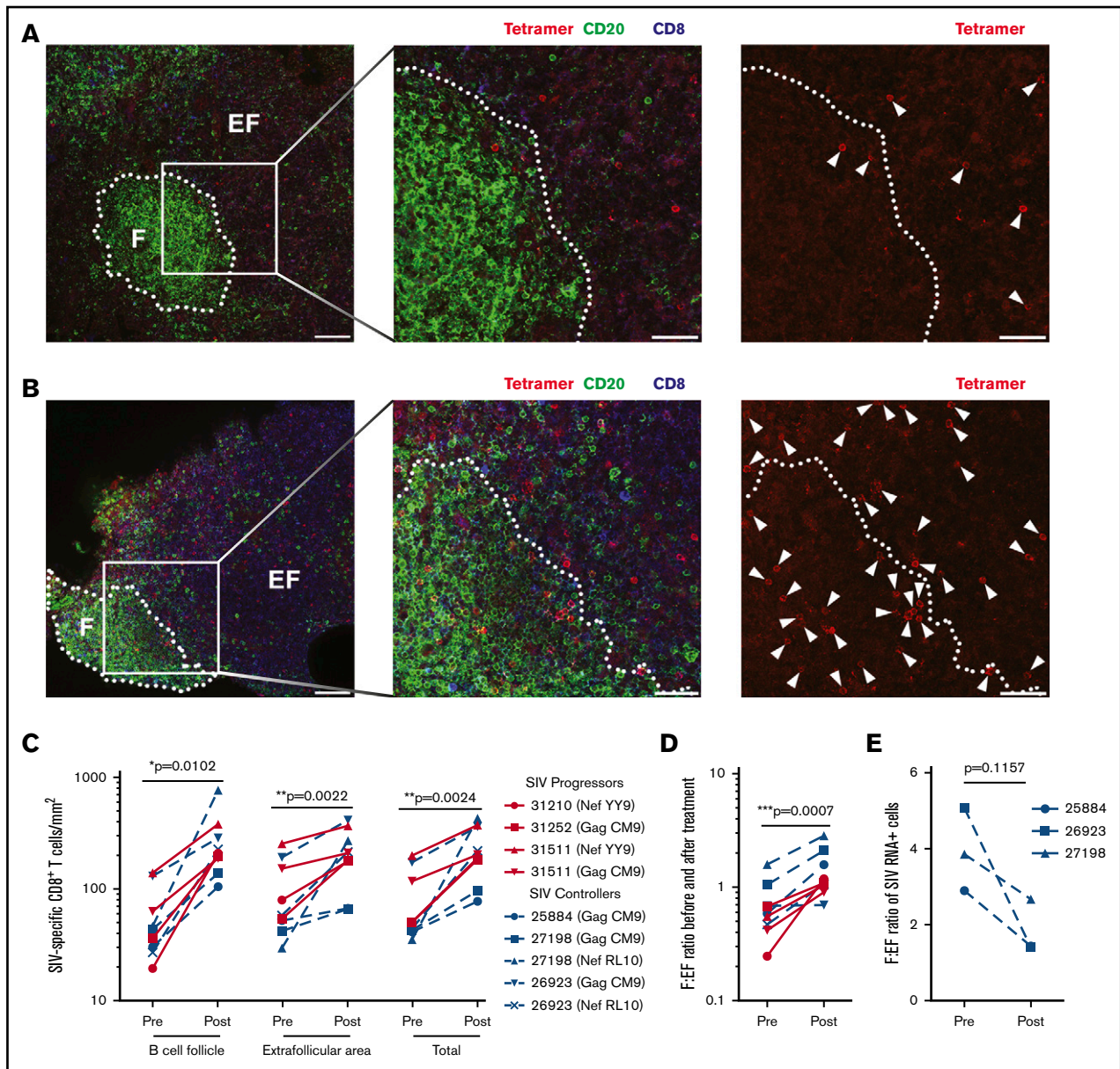
Figure 4. ALT-803 sends SIV-specific CD8$^+$ T cells to the B-cell follicles. SIV-infected RMs received 100 μg/kg of ALT-803. Lymph nodes were sampled before ALT-803 treatment and 5 days posttreatment. (A-B) Representative images of Mamu-A*01 Gag$_{181-189}$CM9-specific tetramer–positive cells (red), CD20$^+$ cells (green), and CD8$^+$ cells (blue) in lymph node sections taken from SIV-infected animal 31252 (A) before and (B) 5 days after ALT-803 treatment. CD20 staining is used to define B-cell follicles (F) and extrafollicular regions (EF) outside B-cell follicles. The images on the far right show the same field as presented in the middle panel with only the red tetramer staining shown. Each tetramer-binding cell is indicated with a white arrow. In panels A and B, scale bars indicate 100 μm (left panels) and 50 μm (2 enlarged right panels). (C) Numbers of tetramer-positive CD8$^+$ T cells per millimeter squared inside and outside of the B-cell follicle as well as total tissue before and after ALT-803 treatment. Animal identification numbers and the MHC-I tetramer used are indicated for both SIV progressors (red solid lines) and controllers (dashed blue lines). (D) F:EF ratio of tetramer-positive CD8$^+$ T cells per millimeter squared before and after ALT-803 treatment. (E) F:EF ratio of SIV-producing cells evaluated via RNAscope analysis in lymph nodes of SIV-infected RMs before and after ALT-803 treatment. (C-E) *P < .05; **P < .01; ***P < .001.

causes SIV-specific CD8$^+$ T cells to migrate from the blood to the lymph nodes, where they then enter B-cell follicles via upregulation of CXCR5. Thus, a new immunotherapeutic exists to bring potent antiviral CD8$^+$ T cells into close proximity to latent viruses residing in B-cell follicles.

In conclusion, we have shown that ALT-803 exhibits pleiotropic effects ideal for HIV eradication strategies. The data presented here

demonstrate that ALT-803 upregulates CXCR5, allowing SIV-specific CD8$^+$ T cells to enter B-cell follicles and consequently decrease the number of SIV-producing cells. Coupled with recent data that ALT-803 reverses viral latency in vitro,[17] it could potentially mediate both the "shock" and the "kill" in eradication strategies. Finally, given that ALT-803 also potently activates NK cells and increases their cytolytic potential,[14,16] it could also be combined

with broadly neutralizing antibodies to mobilize both cytotoxic CD8^{+} T-cell– and NK-mediated antibody-dependent cell-mediated cytotoxicity to clear latent virus. Cumulatively, these 3 effects suggest that ALT-803 is a formidable addition to the HIV eradication armament.

Authorship

Contribution: R.B.J., E.K.J., H.C.W., and J.B.S. conceived the study; and G.M.W., S.L., G.W., J.M.G., J.M.F., J.S.R., J.J.S., A.W.L., T.H., L.D.M., B.S.P., J.B.W., D.F.N., R.B.J., E.C., and P.J.S. generated and analyzed the data and helped write the paper.

Conflict-of-interest disclosure: E.K.J. and H.C.W. are employees of Altor Bioscience Corporation. The remaining authors declare no competing financial interests.

Correspondence: Jonah B. Sacha, Oregon Health & Science University, 505 SW 185th Ave, Beaverton, OR 97006; e-mail: sacha@ohsu.edu; and Pamela J. Skinner, University of Minnesota, 1971 Commonwealth Ave, St. Paul, MN; e-mail: skinn002@umn.edu.

References

1. Connick E, Mattila T, Folkvord JM, et al. CTL fail to accumulate at sites of HIV-1 replication in lymphoid tissue. *J Immunol*. 2007;178(11):6975-6983.

2. Connick E, Folkvord JM, Lind KT, et al. Compartmentalization of simian immunodeficiency virus replication within secondary lymphoid tissues of rhesus macaques is linked to disease stage and inversely related to localization of virus-specific CTL. *J Immunol*. 2014;193(11):5613-5625.

3. Leong YA, Chen Y, Ong HS, et al. CXCR5(+) follicular cytotoxic T cells control viral infection in B cell follicles. *Nat Immunol*. 2016;17(10):1187-1196.

4. He R, Hou S, Liu C, et al. Follicular CXCR5-expressing CD8(+) T cells curtail chronic viral infection. *Nature*. 2016;537(7620):412-428.

5. Fukazawa Y, Lum R, Okoye AA, et al. B cell follicle sanctuary permits persistent productive simian immunodeficiency virus infection in elite controllers. *Nat Med*. 2015;21(2):132-139.

6. Banga R, Procopio FA, Noto A, et al. PD-1(+) and follicular helper T cells are responsible for persistent HIV-1 transcription in treated aviremic individuals. *Nat Med*. 2016;22(7):754-761.

7. Zhu X, Marcus WD, Xu W, et al. Novel human interleukin-15 agonists. *J Immunol*. 2009;183(6):3598-3607.

8. Rhode PR, Egan JO, Xu W, et al. Comparison of the superagonist complex, ALT-803, to IL15 as cancer immunotherapeutics in animal models. *Cancer Immunol Res*. 2016;4(1):49-60.

9. Xu W, Jones M, Liu B, et al. Efficacy and mechanism-of-action of a novel superagonist interleukin-15: interleukin-15 receptor αSu/Fc fusion complex in syngeneic murine models of multiple myeloma. *Cancer Res*. 2013;73(10):3075-3086.

10. Lugli E, Goldman CK, Perera LP, et al. Transient and persistent effects of IL-15 on lymphocyte homeostasis in nonhuman primates. *Blood*. 2010;116(17):3238-3248.

11. Picker LJ, Reed-Inderbitzin EF, Hagen SI, et al. IL-15 induces CD4 effector memory T cell production and tissue emigration in nonhuman primates. *J Clin Invest*. 2006;116(6):1514-1524.

12. Chun TW, Davey RT Jr, Engel D, Lane HC, Fauci AS. Re-emergence of HIV after stopping therapy. *Nature*. 1999;401(6756):874-875.

13. Vandergeeten C, Fromentin R, DaFonseca S, et al. Interleukin-7 promotes HIV persistence during antiretroviral therapy. *Blood*. 2013;121(21):4321-4329.

14. Rosario M, Liu B, Kong L, et al. The IL-15-based ALT-803 complex enhances FcγRIIIa-triggered NK cell responses and in vivo clearance of B cell lymphomas. *Clin Cancer Res*. 2016;22(3):596-608.

15. Kim PS, Kwilas AR, Xu W, et al. IL-15 superagonist/IL-15RαSushi-Fc fusion complex (IL-15SA/IL-15RαSu-Fc; ALT-803) markedly enhances specific subpopulations of NK and memory CD8+ T cells, and mediates potent anti-tumor activity against murine breast and colon carcinomas. *Oncotarget*. 2016;7(13):16130-16145.

16. Seay K, Church C, Zheng JH, et al. In vivo activation of human NK cells by treatment with an interleukin-15 superagonist potently inhibits acute in vivo HIV-1 infection in humanized mice. *J Virol*. 2015;89(12):6264-6274.

17. Jones RB, Mueller S, O'Connor R, et al. A subset of latency-reversing agents expose HIV-infected resting CD4+ T-cells to recognition by cytotoxic T-lymphocytes. *PLoS Pathog*. 2016;12(4):e1005545.

18. Sowell RT, Goldufsky JW, Rogozinska M, et al. IL-15 complexes induce migration of resting memory CD8 T cells into mucosal tissues. *J Immunol*. 2017;199(7):2536-2546.

19. Vinuesa CG, Cyster JG. How T cells earn the follicular rite of passage. *Immunity*. 2011;35(5):671-680.